nature neuroscience

Article

https://doi.org/10.1038/s41593-023-01289-5

The cholinergic basal forebrain provides a parallel channel for state-dependent sensory signaling to auditory cortex

In the format provided by the authors and unedited

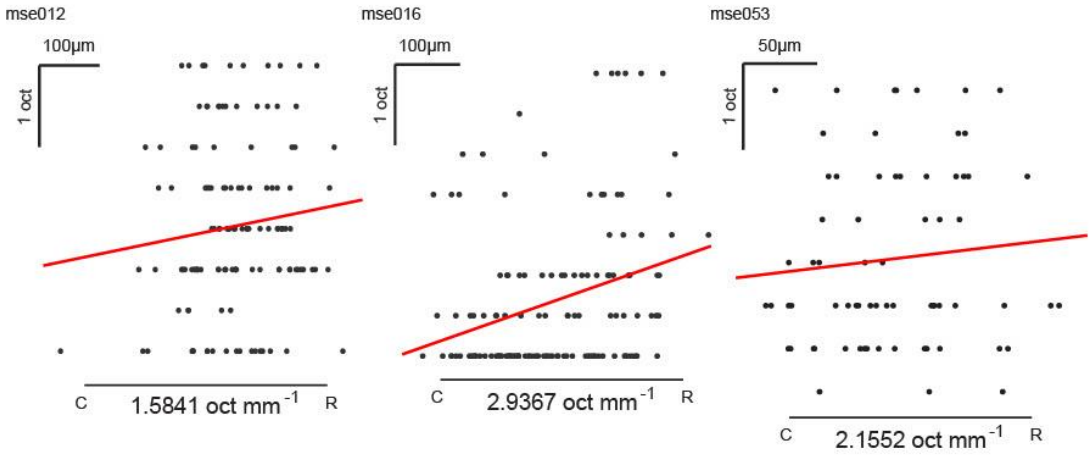

Supplementary Fig. 1 Verification that stereotaxic coordinates of imaging site include primary auditory cortex. Cortical tonotopy measured from jRGECO1a-expressing neurons in 3 animals. Progression of best frequency of neurons in imaging sites along the rostro-caudal axis. Each gray dot indicates the best frequency of a neuron in frequency space (y-axis) projected onto the rostro-caudal axis (x-axis). Slope of line of best fit (red line) reflects progression of best frequency. All 3 sites display cortical tonotopy expected from primary auditory cortex.

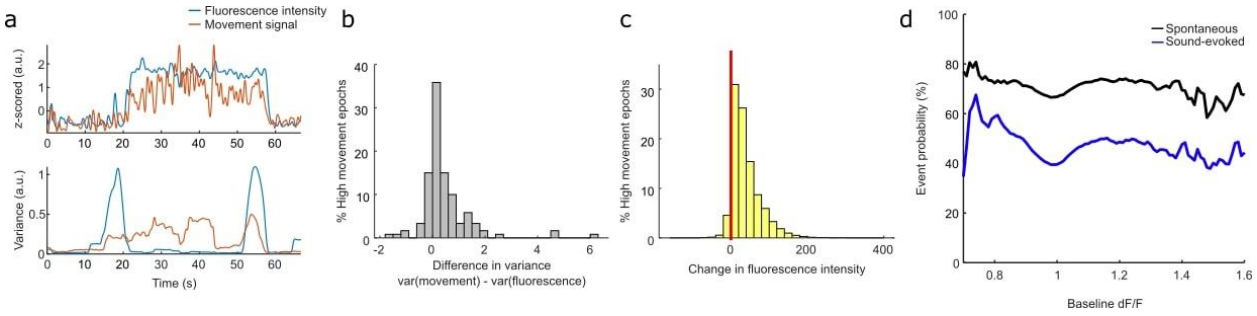

Supplementary Fig. 2 Tonic modulation of sensory cholinergic signals is not an artifact of movement or fluorescence saturation (**a**) Top: Example traces of fluorescence intensity and movement during one recording epoch. Bottom: variance in fluorescence intensity and movement signal of the example traces. Variance in movement signal is greater than variance in fluorescence intensity during movement bouts. (**b**) Histogram of difference in variance of movement signal and fluorescence intensity during epochs with high movement detected. There are more epochs with higher variance in movement than fluorescence intensity. (**c**) Distribution of changes in fluorescence intensity during epochs with high movement. Left of red vertical line indicates decrease in fluorescence intensity during movement and right of red vertical line indicates increase in fluorescence intensity. Equal distribution to the left and right of the red line is expected if change in fluorescence intensity is a result of axons moving in and out of plane during movement. (**d**) Quantification of spontaneous (black) and sound-evoked (blue) fluorescence event probability at different tonic levels. Probability of spontaneous events is greater than probability for sound-evoked events at all tonic levels, strongly suggesting that GCaMP signal is not saturated at higher tonic levels.

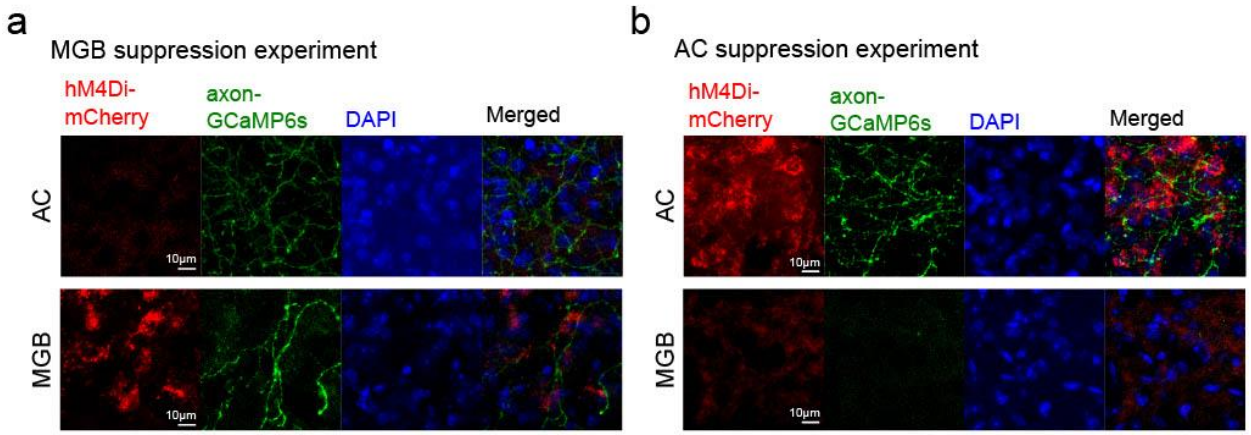

Supplementary Fig. 3 Immunohistochemistry for medial geniculate body and auditory cortex DREADDs targeting. (**a**) Immunohistochemistry for medial geniculate body targeting. Top: auditory cortex imaged for inhibitory DREADDs hM4Di (red), axon-GCaMP6s (green), and DAPI. Bottom: medial geniculate body stained for inhibitory DREADDs hM4Di (red), axon-GCaMP6s (green), and DAPI. Immunohistochemistry is validated in 4 experimental animals. (**b**) Immunohistochemistry for auditory cortex DREADDs targeting. Top: auditory cortex imaged for inhibitory DREADDs hM4Di (red), axon-GCaMP6s (green), and DAPI. Bottom: medial geniculate body stained for inhibitory DREADDs hM4Di (red), axon-GCaMP6s (green), and DAPI. Immunohistochemistry is validated in 2 experimental animals.

Supplementary Table 1: Animal Use Summary

Mouse ID	Genotype	Injections	Experiments
mse011	ChAT-IRES-Cre$^{+/+}$	FLEx-axon-GCaMP6s; jRGECO1a	Figure 1, 2, 5, Ext. Fig. 2, 4, 5, 6, 10, Supp. Fig. 2
mse012	ChAT-IRES-Cre$^{+/+}$	FLEx-axon-GCaMP6s; jRGECO1a	Figure 1, 2, 3f-i, 5, Ext. Fig. 2, 4, 5, 6, 8, 10, Supp. Fig. 1, 2
mse014	ChAT-IRES-Cre$^{+/+}$	FLEx-axon-GCaMP6s; jRGECO1a	Figure 1, 2, 5, Ext. Fig. 1, 2, 4, 5, 6, 10, Supp. Fig. 2
mse016	ChAT-IRES-Cre$^{+/+}$	FLEx-axon-GCaMP6s; jRGECO1a	Figure 1, 2, 3, 5, Ext. Fig. 2, 4, 5, 6, 8, 10, Supp. Fig. 1, 2
mse017	ChAT-IRES-Cre$^{+/+}$	FLEx-axon-GCaMP6s; jRGECO1a	Figure 1, 2, 3, 5, Ext. Fig. 1, 2, 4, 5, 6, 8, 10, Supp. Fig. 2
mse048	ChAT-IRES-Cre$^{+/-}$; Thy1:-jRGECO1a	FLEx-axon-GCaMP6s	Figure 1, 2, 3f-i, 5, Ext. Fig. 2, 4, 6, 8, 10, Supp. Fig. 2
mse050	ChAT-IRES-Cre$^{+/-}$; Thy1:-jRGECO1a	FLEx-axon-GCaMP6s	Figure 1, 2, 3f-i, 5, Ext. Fig. 2, 4, 6, 8, 10, Supp. Fig. 2
mse053	ChAT-IRES-Cre$^{+/+}$; Thy1:-jRGECO1a	FLEx-axon-GCaMP6s	Figure 1, 2, 3f-i, 5, Ext. Fig. 2, 4, 5, 6, 8, 10, Supp. Fig. 1, 2
mse076	ChAT-IRES-Cre$^{+/+}$	FLEx-axon-GCaMP6s; hM4D(Gi)	Figure 4e-h, Supp. Fig. 3b
mse078	ChAT-IRES-Cre$^{+/+}$	FLEx-axon-GCaMP6s; hM4D(Gi)	Figure 4e-h, Supp. Fig. 3b
mse079	ChAT-IRES-Cre$^{+/+}$	FLEx-axon-GCaMP6s; hM4D(Gi)	Figure 4e-h
mse097	ChAT-IRES-Cre$^{+/+}$	FLEx-axon-GCaMP6s; hM4D(Gi)	Figure 4e-h
mse098	ChAT-IRES-Cre$^{+/+}$	FLEx-axon-GCaMP6s; hM4D(Gi)	Figure 4e-h
mse090	ChAT-IRES-Cre$^{+/+}$	FLEx-axon-GCaMP6s; hM4D(Gi)	Figure 4a-d, Supp. Fig. 3a
mse091	ChAT-IRES-Cre$^{+/+}$	FLEx-axon-GCaMP6s; hM4D(Gi)	Figure 4a-d, Supp. Fig. 3a
mse092	ChAT-IRES-Cre$^{+/+}$	FLEx-axon-GCaMP6s; hM4D(Gi)	Figure 4a-d, Supp. Fig. 3a
mse111	ChAT-IRES-Cre$^{+/+}$	FLEx-axon-GCaMP6s; hM4D(Gi)	Figure 4a-d, Supp. Fig. 3a
mse081	ChAT-IRES-Cre$^{+/+}$	GCaMP6f; hM4D(Gi)	Ext. Fig. 9a-c
mse085	ChAT-IRES-Cre$^{+/+}$	GCaMP6f; hM4D(Gi)	Ext. Fig. 9a-c
mse082	ChAT-IRES-Cre$^{+/+}$	GCaMP6f; hM4D(Gi)	Ext. Fig. 9d-f

mse083	ChAT-IRES-Cre$^{+/+}$	GCaMP6f; hM4D(Gi)	Ext. Fig. 9d-f
mse101	ChAT-IRES-Cre$^{+/+}$	FLEx-axon-GCaMP6s	Ext. Fig. 1, 3, 9g-l, 4
mse102	ChAT-IRES-Cre$^{+/+}$	FLEx-axon-GCaMP6s	Ext. Fig. 1, 3, 9g-l, 4
mse103	ChAT-IRES-Cre$^{+/+}$	FLEx-axon-GCaMP6s	Ext. Fig. 1, 3, 9g-l, 4
mse134	ChAT-IRES-Cre$^{+/+}$	FLEx-axon-GCaMP6s	Ext. Fig. 1
mse194	ChAT-IRES-Cre$^{+/+}$	FLEx-axon-GCaMP6s; DIO-hM4D(Gi)	Ext. Fig. 4
mse195	ChAT-IRES-Cre$^{+/+}$	FLEx-axon-GCaMP6s; DIO-hM4D(Gi)	Ext. Fig. 4
mse217	C57/B6	GCaMP6f	Ext. Fig. 7
mse236	C57/B6	GCaMP6f	Ext. Fig. 7
mse237	C57/B6	GCaMP6f	Ext. Fig. 7
mse244	C57/B6	GCaMP6f	Ext. Fig. 7